The M33 G Protein-Coupled Receptor Encoded by Murine Cytomegalovirus Is Dispensable for Hematogenous Dissemination but Is Required for Growth within the Salivary Gland

Fabiola M. Bittencourt,[a] Shu-En Wu,[a] James P. Bridges,[b] William E. Miller[a]

Department of Molecular Genetics, Biochemistry, and Microbiology, University of Cincinnati College of Medicine, Cincinnati, Ohio, USA[a]; Perinatal Institute, Division of Pulmonary Biology, Cincinnati Children's Hospital Medical Center, Cincinnati, Ohio, USA[b]

ABSTRACT

Human cytomegalovirus (HCMV) is a pathogen found worldwide and is a serious threat to immunocompromised individuals and developing fetuses. Due to the species specificity of cytomegaloviruses, murine cytomegalovirus (MCMV) has been used as a model for *in vivo* studies of HCMV pathogenesis. The MCMV genome, like the genomes of other beta- and gammaherpesviruses, encodes G protein-coupled receptors (GPCRs) that modulate host signaling pathways presumably to facilitate viral replication and dissemination. Among these viral receptors, the M33 GPCR carried by MCMV is an activator of CREB, NF-κB, and phospholipase C-β signaling pathways and has been implicated in aspects of pathogenesis *in vivo*, including persistence in the salivary glands of BALB/c mice. In this study, we used immunocompetent nonobese diabetic (NOD) and immunocompromised NOD-scid-gamma (NSG) mice to further investigate the salivary gland defect exhibited by M33 deficiency. Interestingly, we demonstrate that virus with an M33 deletion (ΔM33) can replicate in the salivary gland of immunocompromised animals, albeit with a 400-fold growth defect compared with the growth of wild-type virus. Moreover, we determined that M33 does not have a role in cell-associated hematogenous dissemination but is required for viral amplification once the virus reaches the salivary gland. We conclude that the reduced replicative capacity of the ΔM33 virus is due to a specific defect occurring within the localized environment of the salivary gland. Importantly, since the salivary gland represents a site essential for persistence and horizontal transmission, an understanding of the mechanisms of viral replication within this site could lead to the generation of novel therapeutics useful for the prevention of HCMV spread.

IMPORTANCE

Human cytomegalovirus infects the majority of the American people and can reside silently in infected individuals for the duration of their lives. Under a number of circumstances, the virus can reactivate, leading to a variety of diseases in both adults and developing babies, and therefore, identifying the function of viral proteins is essential to understand how the virus spreads and causes disease. We aim to utilize animal models to study the function of an important class of viral proteins termed G protein-coupled receptors with the ultimate goal of developing inhibitors to these proteins that could one day be used to prevent viral spread.

Cytomegaloviruses (CMVs) belong to the betaherpesvirus family and cause a lifelong infection within their host organism. Human cytomegalovirus (HCMV) is found ubiquitously, and 50 to 80% of the world's population is HCMV seropositive (1). In immunocompetent individuals, HCMV infection causes only mild symptoms; however, HCMV infection is a significant cause of morbidity in patients with a compromised or immature immune system, including preterm and newborn babies. Infection of the developing fetus, commonly referred to as congenital infection, can lead to neurological impairment and hearing loss (2–4). Primary infection or reactivation of latent virus in immunocompromised transplant patients can have devastating consequences, including organ failure and diseases of the gastrointestinal tract (5, 6).

CMVs show strict species specificity, which has severely restricted *in vivo* studies of HCMV pathogenesis, as the virus is unable to replicate and disseminate in model organisms like the mouse. For this reason, murine cytomegalovirus (MCMV) has commonly been used as a model system to study aspects of CMV pathogenesis *in vivo*, and this model has been particularly useful for uncovering viral mechanisms responsible for immunomodu-

lation as well as defining factors involved in viral dissemination (7–10). Acute CMV infection in immunocompetent mice is characterized by robust viral replication in internal organs, such as the liver and spleen, within 2 to 3 days postinfection, followed by secondary dissemination of this newly produced virus to additional organs, such as the salivary gland (11–13). Studies have shown that virus produced in endothelial cells, presumably in the spleen, is the virus that ultimately reaches secondary sites, such as the salivary gland (14, 15). MCMV replicates within the acinar epithelium of the salivary gland, spreads via the well-organized series of ducts connecting the individual acini, and is eventually shed into the saliva (16–18). Salivary glands are important sites for

horizontal transmission, as the virus can be detected in the saliva of both humans and mice for prolonged periods of time ([16], [19]). In the case of MCMV, the virus can persist in the salivary glands for months before eventually being cleared by $CD4^+$ T cell responses ([20–23]).

Viruses utilize an extensive array of viral and host genes to control and direct viral movement from the portal of entry to sites of horizontal transmission. The cytomegaloviruses encode several proteins that are not absolutely essential for replication *in vitro* but play critical roles in viral replication, trafficking, and growth within important tissues *in vivo* ([24–27]). One such protein is the MCMV-encoded G protein-coupled receptor (GPCR) homolog M33 ([28]). In terms of molecular signaling capacity, M33 appears to be a functional homolog of the HCMV US28 protein, as M33, like US28, appears to constitutively activate the $G\alpha_q/G\alpha_{11}$ subfamily of heterotrimeric G proteins. M33 and US28 both activate a number of signaling molecules and transcription factors downstream of $G\alpha_q/G\alpha_{11}$, including phospholipase C (PLC-β), protein kinase C (PKC), nuclear factor kappa light-chain enhancer of activated B cells (NF-κB), nuclear factor of activated T cells (NF-AT), and cyclic AMP response element binding protein (CREB) ([29–32]). M33 is not essential for replication in fibroblasts in tissue culture or for replication at sites of acute infection *in vivo*, such as the spleen and liver ([29], [33], [34]). However, MCMV mutants deficient in M33 (ΔM33) exhibit severe growth defects in the salivary glands of immunocompetent BALB/c mice, and there is some evidence that M33 may affect immune clearance, as one report demonstrates that ΔM33 viruses are cleared more efficiently in BALB/c mice ([29], [33–36]). It remains unclear if M33 functions to (i) prevent viral clearance mediated by innate or adaptive immunity, (ii) facilitate viral dissemination from visceral organs to the salivary gland, or (iii) support viral amplification and spread within the salivary gland itself. Our overall goals are to define the functional activity of M33 *in vivo* and to characterize the molecular mechanisms that facilitate this activity.

While previous studies with MCMV M33 have used the prototypical mouse strain BALB/c, we hypothesized that the nonobese diabetic (NOD)-scid gamma (NSG) mouse strain would be useful for investigating several of the points raised above. NSG mice are defective in the development of B and T cell responses due to mutation in the *Prkdc^scid* gene, a critical component of the variable(diversity)joining [V(D)J] recombination system, and NSG mice are extremely defective in NK and other innate immune responses due to deletion of the interleukin-2 (IL-2) receptor common gamma chain of the interleukin 2 receptor, which is required for high-affinity signaling via the IL-2, IL-4, IL-7, IL-9, IL-15, and IL-21 cytokine receptors ([37–39]). Utilizing the NSG animals would enable us to determine if M33-directed evasion of immune-mediated MCMV clearance plays a central role in dissemination of MCMV to the salivary gland. Moreover, we hypothesized that infection of immunocompromised NSG animals would lead to higher and more sustained virus titers in primary organs and blood, perhaps leading to the increased movement of ΔM33 virus to the salivary glands and thus enabling us to compare wild-type and ΔM33 virus growth within the gland.

Using the immunocompromised NSG mouse model, we demonstrate that M33-null virus can in fact replicate in the salivary gland, although it exhibits a 3- to 4-log-unit growth defect compared to the growth of wild-type MCMV. We determined that the growth defect exhibited by ΔM33 viruses occurs within the sub-

structure of the salivary gland itself, as ΔM33 viruses exhibited normal levels of hematogenous dissemination and entered the salivary gland. This defect in growth within the gland was demonstrated using high-dose intraperitoneal (i.p.) infection and direct intraglandular injections. Finally, we used green fluorescent protein (GFP)-tagged viruses to examine viral spread within the salivary gland *in vivo* and in freshly isolated salivary gland explants *in vitro*. From these studies, we conclude that the ΔM33 virus exhibits an interacinar spread defect *in vivo*, thus preventing efficient growth within the gland. Considering that the salivary glands are an important site for horizontal transmission, further elucidation of the parameters that affect salivary gland growth could ultimately be exploited to design novel inhibitors of CMV transmission.

MATERIALS AND METHODS

Tissue culture cell lines and primary salivary gland explants. NIH 3T3 cells were purchased from ATCC and maintained at 37°C in 5% CO_2 and Dulbecco modified Eagle's medium (DMEM) supplemented with 10% newborn calf serum and penicillin-streptomycin. Salivary gland (i.e., submandibular) explants were generated by harvesting glands from 3- to 6-week-old C57BL/6 mice. Dissected glands were injected with dispase (Stemcell Technologies) and 0.15% collagenase type 3 (Worthington) and digested for 20 min at 37°C in 2 ml of the dispase-collagenase solution. The glands were gently teased apart with tweezers and incubated for an additional 20 min at 37°C in the dispase-collagenase solution. Dissociated cells were diluted in phosphate-buffered saline (PBS), passed through a 70-μm-pore-size cell strainer, and then washed 3 times in PBS. Cell pellets were resuspended in BEGM bronchial epithelial cell growth medium (containing the supplements from the BEGM bullet kit and 4% charcoal-stripped fetal bovine serum; Lonza). Isolated cells were then plated in 12-well dishes coated with Cultrex basement membrane extract (Trevigen) at a density of approximately 1×10^6 cells per well. Adhered cells were gently washed with PBS at 24 and 48 h postplating and refed after each wash with fresh BEGM growth medium. Adhered cells went through several rounds of cell division, resulting in the appearance of tight clusters each containing 6 to 20 cells by 96 h postplating. Staining of primary salivary gland clusters was carried out at 120 h postisolation, and virus infection was initiated at between 72 and 120 h postisolation. All experiments were carried out in primary cells prior to subculture. All animal procedures were approved by the University of Cincinnati Institutional Animal Care and Use Committee.

Viruses. MCMV K181, ΔM33, and M33FL-RSC viruses were described in an earlier study from the Miller laboratory ([29]). M33-RSC virus was generated by replacing the Flp recombination target (FRT) scar of the ΔM33 virus with M33 genomic sequences containing the M33 intron but without a FLAG tag sequence. Bacteriophage lambda red recombination was used to generate the M33-RSC virus essentially as described in our earlier studies ([29]). Viral stocks were made in NIH 3T3 fibroblasts, and the viral titer was determined via plaque assay. Salivary gland-derived viruses were generated by homogenizing the salivary glands of NSG mice infected with 1×10^6 PFU. Salivary glands were harvested at day 12 postinfection. Using this high dose in NSG animals enabled us to recover salivary gland stocks of the ΔM33 virus at a titer sufficient to be tested for growth in subsequent infection experiments. GFP-tagged viruses were generated via bacteriophage lambda red recombination techniques. A DNA fragment containing GFP under the control of the CMV promoter was inserted into the HindIII L region of bacterial artificial chromosome (BAC)-derived MCMV pARK25 and ΔM33 pARK25 genomes. A kanamycin resistance gene flanked by FRT recombinase sites was used for the selection of recombinants and was subsequently excised using Flp recombinase. Integration was confirmed by restriction digestion. For virus reconstitution, NIH 3T3 cells were transfected with an MCMV bacterial

artificial chromosome and TransIT-LT1 transfection reagent according to the manufacturer's protocol.

Mice. Eight- to 12-week-old nonobese diabetic severe combined immunodeficient, IL-2 common γ chain null (NSG) mice were purchased from Cincinnati Children's Hospital Comprehensive Mouse and Cancer Core. Eight- to 12-week-old NOD mice were purchased from Taconic Farms. Three- to 6-week-old C57BL/6 animals were bred in-house. Mice were kept with food and water *ad libitum*.

Mouse infections. (i) Intraperitoneal infection. NSG and NOD mice were infected intraperitoneally with various doses (1×10^5 to 2×10^6 PFU) of K181, ΔM33, M33 RSC, K181-GFP, or ΔM33-GFP viruses.

(ii) Intra-salivary gland infection. For intra-salivary gland infection, NSG and NOD mice were anesthetized by inhalation of isoflurane, and 1×10^5 PFU of K181 or ΔM33 viruses was injected into each lobe of the submandibular gland.

Organ harvest and homogenizations. Upon sacrifice, blood was collected via cardiac puncture with a syringe and stored in tubes containing 20 μl 7.5% Na_2EDTA. Red blood cells were lysed with red blood cell lysis buffer (4.015 g NH_4Cl, 0.5 g $NaHCO_3$, and 0.0186 g EDTA in 200 ml distilled H_2O), samples were centrifuged to remove cell debris, and peripheral blood leukocytes were isolated and counted. Spleens, livers, and salivary glands were harvested, placed in 250 to 1,000 μl complete DMEM, and stored at −80°C until the organs were thawed and disrupted with a glass homogenizer or tissue grinder.

Plaque assays. Organ homogenates and viral stocks were diluted and used to determine the viral titer on NIH 3T3 cell monolayers in 12-well plates. Infected cell monolayers were overlaid with minimal essential medium containing 10% calf serum, nonessential amino acids, penicillin-streptomycin, and 1.5% carboxymethylcellulose (Sigma). Five days later, the cells were fixed with methanol and stained with 10% Giemsa (Sigma) and the plaques were counted using a dissecting microscope.

Infectious center assays. Splenocytes were isolated by disrupting whole spleens and passing the disrupted spleens through a 70-μm-pore-size nylon cell strainer (BD Falcon), followed by lysis of red blood cells. Peripheral blood leukocytes were isolated as described above. Splenocytes or leukocytes (10,000 to 100,000) were added to an NIH 3T3 cell monolayer and were later covered with overlay medium and carboxymethyl cellulose. Five days later, the cells were fixed with methanol and stained with 10% Giemsa and the plaques were counted using a dissecting microscope.

Viral growth curves and spread of GFP-tagged viruses in primary salivary gland explants. Primary salivary gland explants were infected with wild-type or ΔM33 viruses at a multiplicity of infection (MOI) of 0.1 PFU/cell. All infections were performed in 12-well plates using primary cells at days 3 to 5 postisolation, and the cells were never subcultured. Supernatant samples were collected at days 1 to 4 postinfection, frozen, and later used for viral titer determination via plaque assays in NIH 3T3 fibroblasts, as described above. For visualization of viral infection and spread, primary salivary gland explants were infected with K181-GFP or ΔM33-GFP viruses at an MOI of 0.1 PFU/cell. At days 1 to 3 postinfection, GFP-positive cells were visualized on a Nikon TE2000 inverted microscope equipped with an epifluorescence unit using 450- to 490-nm excitation filters and 520-nm-band-pass emission filters. Images were captured using an Olympus Q Color 5 camera and QCapturePro software.

Immunocytochemistry and confocal microscopy. Salivary glands harvested at 8 or 12 days postinfection were fixed with 4% paraformaldehyde in PBS for 24 h, incubated in 30% sucrose overnight, embedded in OTC compound (Tissue-Tek), and frozen in liquid nitrogen. Sections of 4 μm were used for immunocytochemistry. For M44 and immediate early (IE) protein immunocytochemistry, sections were thawed and staining for the M44 or IE protein was done in several steps with a mouse-on-mouse fluorescence detection kit with the MaxFluor mouse-on-mouse Alexa 488 (MOM-488) reagent, according to the manufacturer's instructions (Max Vision Biosciences). Briefly, endogenous immunoglobulins were blocked and sections were stained with anti-M44 antibody (provided by J. Shanley), CROMA 101 anti-IE protein antibody (provided by S. Jonjic), or PBS alone as a negative control for 12 h (40, 41). Sections were then stained with the MaxFluor MOM-488 secondary reagent and mounted in antifade medium containing Fluoroshield with DAPI (4′,6-diamidino-2-phenylindole; Sigma). For GFP immunocytochemistry, frozen sections of infected salivary glands with GFP-tagged K181 or GFP-tagged M33 were used for determination of GFP expression. For E-cadherin and ZO-1 staining of salivary gland explant clusters, cells were fixed in 4% paraformaldehyde, permeabilized in 0.05% Tween 20, and stained with anti-E-cadherin (catalog number MAB7481; R&D Systems) or anti-ZO-1 (catalog number sc-33725; Santa Cruz) antibodies, followed by staining with species-specific secondary antibodies. Stained sections or cells were mounted in antifade medium containing Fluoroshield with DAPI (Sigma) or ProLong Gold antifade reagent with DAPI (Life Technologies). Experiments examining M44, IE protein, and GFP expression were performed on a Zeiss LSM510 NLO two-photon microscope with a water immersion ×40/1.2 C-Apochromat objective. Images for ZO-1 and E-cadherin were obtained on a Nikon A1+ inverted confocal microscope with a ×60 water objective.

Reverse transcription (RT)-PCR analysis. Dissected salivary glands or day 5 salivary gland explant clusters were solubilized in RNA-BEE (Tel-Test, Inc.), and RNA was extracted according to the manufacturer's recommendation. First-strand cDNA was synthesized from 1 μg total RNA using an iScript cDNA synthesis kit (Bio-Rad Laboratories). PCR amplification of cDNA was performed in an Eppendorf Mastercycler apparatus using 25 cycles (for β-actin) or 30 cycles (for amylase 1 [Amy1] and aquaporin 5 [AQP5]). The primers used were Aqp5-FOR (CTCTGCATCTTCTCCTCCACG) and Aqp5-REV (TCCTCTCTATGA TCTTCCCAG) for aquaporin 5 amplification, Amylase1-FOR (GGTGC AACAATGTTGGTGTC) and Amylase1-REV (ACTGCTTTGTCCAGCT TGAG) for amylase 1 amplification, and BACT-FOR (CCTAAGGCCAA CCGTGAAAAG) and BACT-REV (TCTCATGGTGCTAGGAG CCA) for β-actin amplification (42).

RESULTS

M33 is required for MCMV growth in the salivary glands of immunocompetent NOD and immunocompromised NSG mice. Salivary glands are seeded late during infection and are an important site for CMV persistence (16, 19). Virus particles can be detected in the salivary gland and saliva long after MCMV has been cleared from other organs, and as such, the salivary glands are frequently used to model aspects of MCMV persistence (16). Previous studies in immunocompetent mouse models have demonstrated that M33-null viruses replicate normally in primary sites of replication, such as the spleen and liver, but are profoundly defective for growth in the mouse salivary gland (28, 29, 34). These data indicate that some step in the virus life cycle subsequent to replication in the primary organs (e.g., the spleen) requires M33 signaling activity. We chose to use the nonobese diabetic (NOD) mouse strain and its immunodeficient derivative, NOD-scid-gamma (NSG), to further examine the role that M33 plays in promoting viral growth in the salivary gland.

Intraperitoneal infection of NOD mice with 1×10^6 PFU of wild-type MCMV (K181) or MCMV with an M33 deletion (ΔM33) resulted in an initial phase of replication where both viruses could be detected at similar levels in spleen and liver (Fig. 1A, top and middle). The viruses were subsequently cleared from the spleen and liver by 14 days postinfection (Fig. 1A, bottom). Little to no virus was detectable in the salivary gland at 4 days postinfection (Fig. 1A, top), while wild-type K181 but not ΔM33 virus was detectable in the salivary gland at 7 and 14 days postinfection (Fig. 1A, middle). Similar results were obtained following a low-dose i.p. infection with 1×10^5 PFU (Fig. 1B). These experiments in-
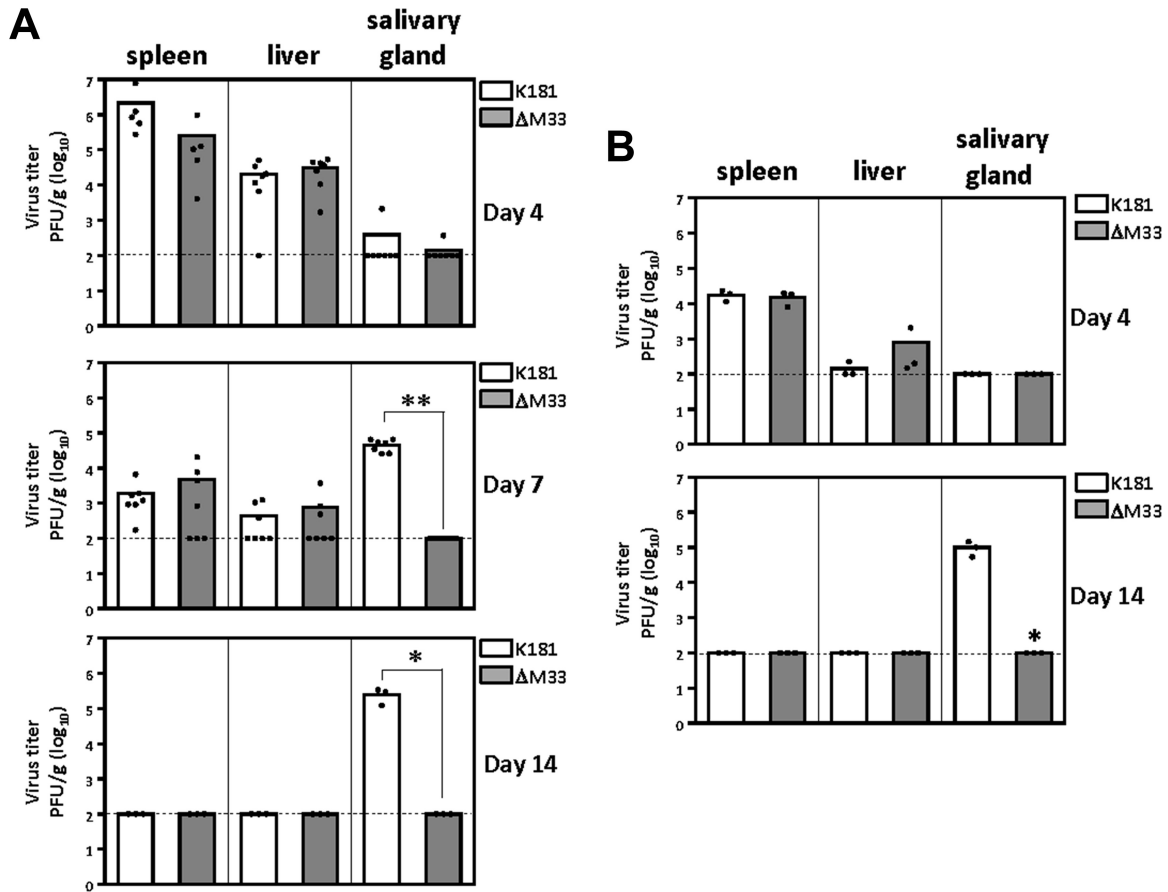
FIG 1 MCMV ΔM33 exhibits normal replication in the spleen and liver but exhibits severely restricted replication in the salivary gland of NOD mice. (A) NOD mice were infected intraperitoneally with 1×10^6 PFU of wild-type or ΔM33 K181 MCMV. At days 4, 7, and 14 postinfection, spleens, livers, and salivary glands were harvested and homogenized with a tissue grinder. (B) Experiments were performed as described in the legend to panel A, except that infections were done with 1×10^5 PFU per animal and organs were harvested on days 4 and 14. Dilutions of the organ homogenates were used for viral titer determination via plaque assay on NIH 3T3 cell monolayers. Each symbol represents one animal. Dashed lines, the limit of detection. Statistical analyses were performed using an unpaired *t* test. *, $P < 0.05$; **, $P < 0.01$.

dicate that the salivary gland phenotype of the ΔM33 virus that was previously observed in BALB/c mice (28, 29, 33) is similarly manifested in the unrelated NOD strain of mice, indicating that the M33 phenotype is a general phenomenon in immunocompetent mice and not restricted to the genetic background of BALB/c mice. Moreover, in these experiments, the wild-type and ΔM33 viruses cleared equally well from the spleen and liver, suggesting that the M33 salivary gland phenotype is not due to clearance of virus from tissues typically affected during acute infection.

We next sought to examine the replication of K181 and ΔM33 viruses in immunodeficient NSG mice to determine if M33 is required for dissemination to and replication within the salivary gland in mice unable to mount appropriate innate and adaptive immune responses (38, 43). After a low-dose i.p. infection of 1×10^5 PFU, K181 and ΔM33 viruses replicated to similar viral titers in spleen and liver at days 4 to 14 postinfection in the NSG mice (Fig. 2, top and middle). In contrast to the immunocompetent NOD mice, MCMV titers in the spleen and liver continued to rise from days 4 to 14, consistent with the lack of immune control in these animals. When viral growth/replication in the salivary gland at days 4 and 14 postinfection was examined, we again found that the ΔM33 virus was severely defective in its ability to grow in the

salivary gland of the NSG mice (Fig. 2, top and middle). These results indicate that even in the absence of innate or adaptive immune responsiveness, the ΔM33 virus is unable to efficiently grow in the salivary gland, suggesting that M33 does not function solely as an immunosuppressive protein to promote dissemination to the salivary gland. Interestingly, while we were unable to detect any ΔM33 virus in the salivary glands of NOD mice, we did detect low but statistically significant levels of ΔM33 virus in the salivary glands of some NSG mice 14 days after an i.p. infection (Fig. 2A, middle). Since we were able to detect low levels of ΔM33 virus in the salivary glands of some NSG mice at day 14 postinfection, we tested the hypothesis that ΔM33 virus might simply be delayed in its ability to replicate in the salivary gland. To examine this question, we infected NSG mice i.p. with 1×10^5 PFU and analyzed viral growth in the spleen, liver, and salivary gland at 21 days postinfection. Similar to the findings of the studies at day 14, the ΔM33 virus remained severely defective in its ability to grow in the gland when the time point of analysis was carried out to 21 days postinfection (Fig. 2A, bottom). Thus, even if more time is allowed for the establishment of infection, the ΔM33 virus remains defective for efficient viral replication within the salivary gland. To confirm that the phenotype of the ΔM33 virus is due to
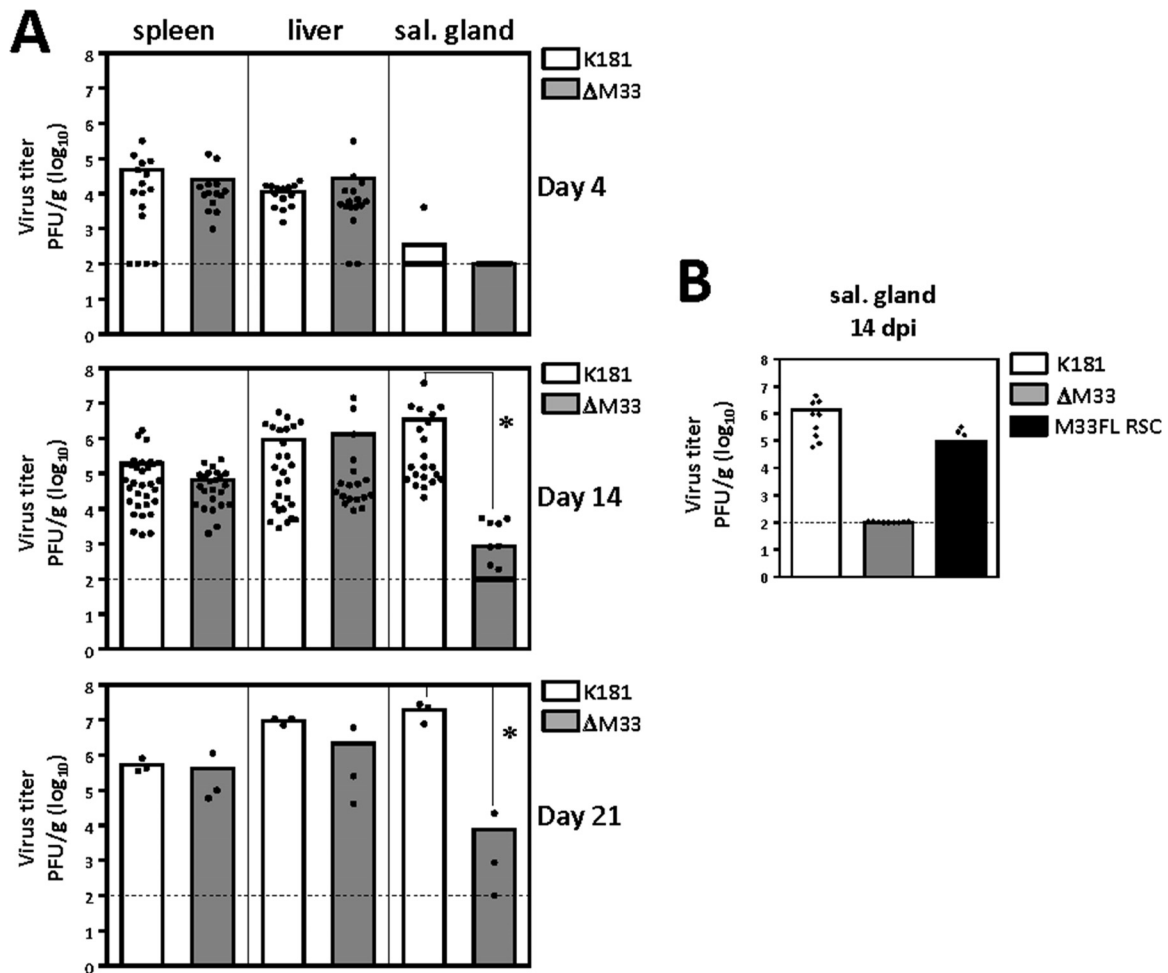
FIG 2 M33 is required for efficient viral growth in the salivary (sal.) gland of immunocompromised NSG mice. NSG mice were infected intraperitoneally with 1×10^5 PFU of the indicated viruses. (A) At 4, 14, and 21 days postinfection (dpi), spleens, livers, and salivary glands were harvested and homogenized with a tissue grinder. Dilutions of the organ homogenates were used for viral titer determination via plaque assay on NIH 3T3 cell monolayers. (B) Replication of a revertant virus was assessed for salivary gland growth. Each symbol represents one animal. Dashed lines, the limit of detection. Statistical analyses were performed using an unpaired *t* test. *, $P < 0.05$.

deletion of the M33 gene, we examined the replication of an M33 revertant virus in the salivary gland of NSG mice at day 14. Experiments with the M33 revertant virus (containing a FLAG-tagged M33 gene in the M33 locus) demonstrated that the defect in viral replication of the ΔM33 virus in the salivary gland is M33 specific, as replication in the salivary gland was restored to levels similar to those of the K181 wild-type virus (Fig. 2B).

M33 is not required for hematogenous dissemination in NSG mice. Based on the findings that the ΔM33 virus is not subjected to faster clearance from the spleen in NOD mice and since the ΔM33 virus phenotype is not rescued in NSG mice, we next sought to determine if ΔM33 and wild-type viruses exhibited similar levels of dissemination via the blood. MCMV infection in mice is thought to occur by an initial dissemination of virus from the entry point to the spleen and liver, followed by abundant replication at these sites and then a second viremia, whereby virus is disseminated via blood leukocytes, ultimately reaching secondary sites of infection, such as the salivary gland (11, 12). To investigate if M33 has a role in viral dissemination, we analyzed MCMV infection and replication in splenocytes and blood leukocytes at sev-

eral days postinfection using infectious center assays (Fig. 3). In these assays, splenocytes or leukocytes from infected animals were cocultured with fibroblast monolayers, and the number of infectious centers that appeared represented the number of productively infected splenocytes or leukocytes. NSG animals were infected with 1×10^6 PFU of K181 or ΔM33 viruses, and splenocytes were isolated via standard procedures. We examined the number of infected splenocytes at days 4, 8, and 12 postinfection and observed that the number of infected splenocytes was similar for both K181 and ΔM33 viruses over all time points examined (Fig. 3A). We next analyzed the number of infected blood leukocytes in mice infected with K181 or ΔM33 virus. Peripheral blood was isolated via cardiac puncture, red blood cells were lysed, and the number of infected blood leukocytes was determined. We observed similar numbers of infected cells for both K181 and ΔM33 viruses at all time points observed (Fig. 3B). We used the higher viral dose (1×10^6 PFU per animal) in these experiments to facilitate more robust detection of infected blood leukocytes, although similar results were obtained using low-dose infection (1×10^5 PFU per animal) (data not shown). The similarities in the number
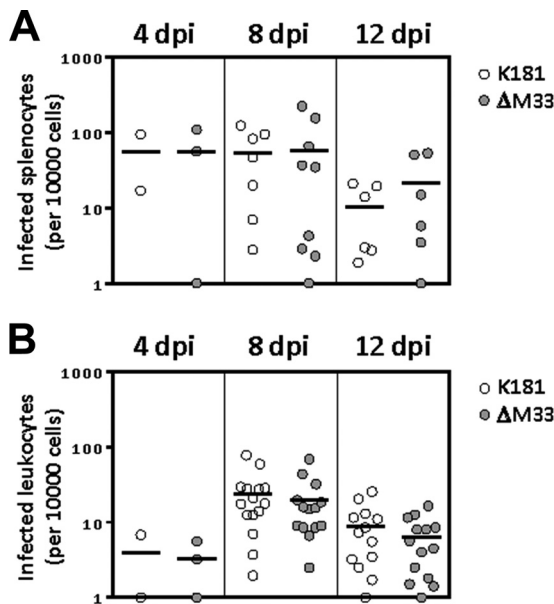
FIG 3 M33 is not required for hematogenous dissemination of MCMV in NSG mice. NSG mice were infected intraperitoneally with 1×10^6 PFU of the indicated viruses. Splenocytes (A) or leukocytes (B) were isolated from spleens or whole blood at 4, 8, and 12 days postinfection. Splenocytes or leukocytes ($n = 10,000$) were then used for infectious center assays by coculturing with NIH 3T3 cell monolayers to determine the number of infected cells in each population. Symbols represent the number of infected cells per animal. Statistical analyses were performed using an unpaired t test.

of infected splenocytes and blood leukocytes between both wild-type K181 and ΔM33 viruses indicate that M33 does not have an important role in viral dissemination inside the immunocompromised host.

High-dose infection in NSG mice indicates that the ΔM33 virus can reach the salivary gland but fails to replicate efficiently once it is in the gland. Since some NSG animals infected with 1×10^5 PFU of ΔM33 virus had low but detectable levels of virus growth in the salivary gland, we surmised that if we used the high infectious dose used in the blood dissemination experiments (1×10^6 PFU per animal), this might allow more robust replication in primary organs, enable more virus to disseminate to the salivary gland, and facilitate studies aimed at understanding the ΔM33 virus phenotype. Although we typically analyzed salivary gland growth at 14 days postinfection (Fig. 1 to 2), the high viral dose used for these experiments led to significant mortality among both mice infected with wild-type virus and mice infected with ΔM33 virus at days 13 to 15 postinfection (data not shown); therefore, we set our longest time point at 12 days postinfection. We also included an additional intermediate time point in order to more closely examine the kinetics of wild-type and ΔM33 virus replication in the salivary glands between 8 and 12 days postinfection. Using this high-dose approach, viral titers reached maximal levels in the spleen (Fig. 4A) and liver (Fig. 4B) by 4 days postinfection and remained high throughout the course of the experiment. Moreover, both K181 and ΔM33 viruses exhibited similar levels of replication at all three time points (Fig. 4A and B). When salivary gland growth was analyzed, we could clearly detect viral growth in the gland at 8 days postinfection with both viruses, while the ΔM33 virus exhibited a mildly defective phenotype (Fig. 4C). At

this intermediate day 8 time point, K181 titers were 2.1×10^5 PFU/g, whereas ΔM33 titers were 2.7×10^4 PFU/g. We observed that K181 exhibited an approximately 3-log-unit increase in viral titers between the 8- and 12-day time points, while the ΔM33 virus exhibited only a modest increase in viral titer of about 1 log unit during this same interval. Importantly, this approach has enabled us to develop a model for examining the role of M33 within the salivary gland once MCMV infection has been established (at 8 days postinfection). Taken together, these results indicate that the ΔM33 virus exhibits a growth defect within the salivary gland of over 400-fold compared to the growth of wild-type K181 (Fig. 4C). Additionally, experiments with an M33 rescue virus demonstrated that this defect in viral replication of the ΔM33 virus in the salivary gland is indeed due to loss of the M33 gene, as this phenotype could be rescued when the M33 gene was repaired (Fig. 4D). Thus, we conclude that while M33 is dispensable for growth in primary sites of infection and dispensable for hematogenous dissemination, it is essential for efficient viral replication within the salivary gland itself.

The ability to recover some ΔM33 virus from the salivary gland of NSG mice (Fig. 4C) provided us with the appropriate reagent to ask whether salivary gland stocks of ΔM33 virus maintain the phenotype of the tissue culture stocks of the ΔM33 virus. Salivary gland-derived virus stocks are more virulent than tissue culture virus stocks due to unknown changes that occur when the virus replicates in the salivary gland *in vivo* (44). In order to determine whether salivary gland-derived stocks of ΔM33 virus would behave differently than tissue culture-derived stocks, we infected NSG mice with 1×10^4 PFU of salivary gland-derived K181 or ΔM33 virus and analyzed viral growth in the spleen, liver, and salivary gland at 14 days postinfection (Fig. 4E). Compared to wild-type K181, the ΔM33 virus remained severely defective in salivary gland growth using this approach, indicating that the changes that occur in MCMV following salivary gland growth do not impact the observed M33 phenotype.

Immunohistochemical analysis indicated that the reduced ΔM33 titers correlate with a reduction in the number of infected cells. Since our data indicate that the ΔM33 virus can reach the salivary gland but replicates with reduced efficiency once it is in the gland, we would expect to find ΔM33 virus-infected cells in the gland, but at a reduced frequency. We used an immunohistochemical approach to explore this question and chose to examine expression of the viral proteins M44 and M123. M44 is a viral polymerase processivity factor that is expressed with delayed early/late kinetics and found in large quantities in the nuclei of infected cells, while M123 is the immediate early protein IE1 (40, 41). Frozen sections of salivary glands infected with a high dose (1×10^6 PFU) of K181 or ΔM33 viruses were stained for M44 expression at 12 days postinfection using an anti-M44 monoclonal antibody (MAb) and mouse-on-mouse Alexa 488 reagent (MOM-488) (Fig. 5A, anti-M44/MOM-488). Salivary glands from infected animals stained with the secondary MOM-488 reagent alone (Fig. 5A, MOM-488 Alone) or salivary glands from mock-infected animals stained with anti-M44 and MOM-488 (data not shown) were included as controls. M44-positive cells were quantified using NIH ImageJ software (Fig. 5B). In animals infected with wild-type K181, we observed M44 expression in $\sim$2% of DAPI-stained cells (10 in 500), while in animals infected with ΔM33, we observed M44 expression in $\sim$0.2% of DAPI-stained cells (1 in 500). Similar results were obtained when using
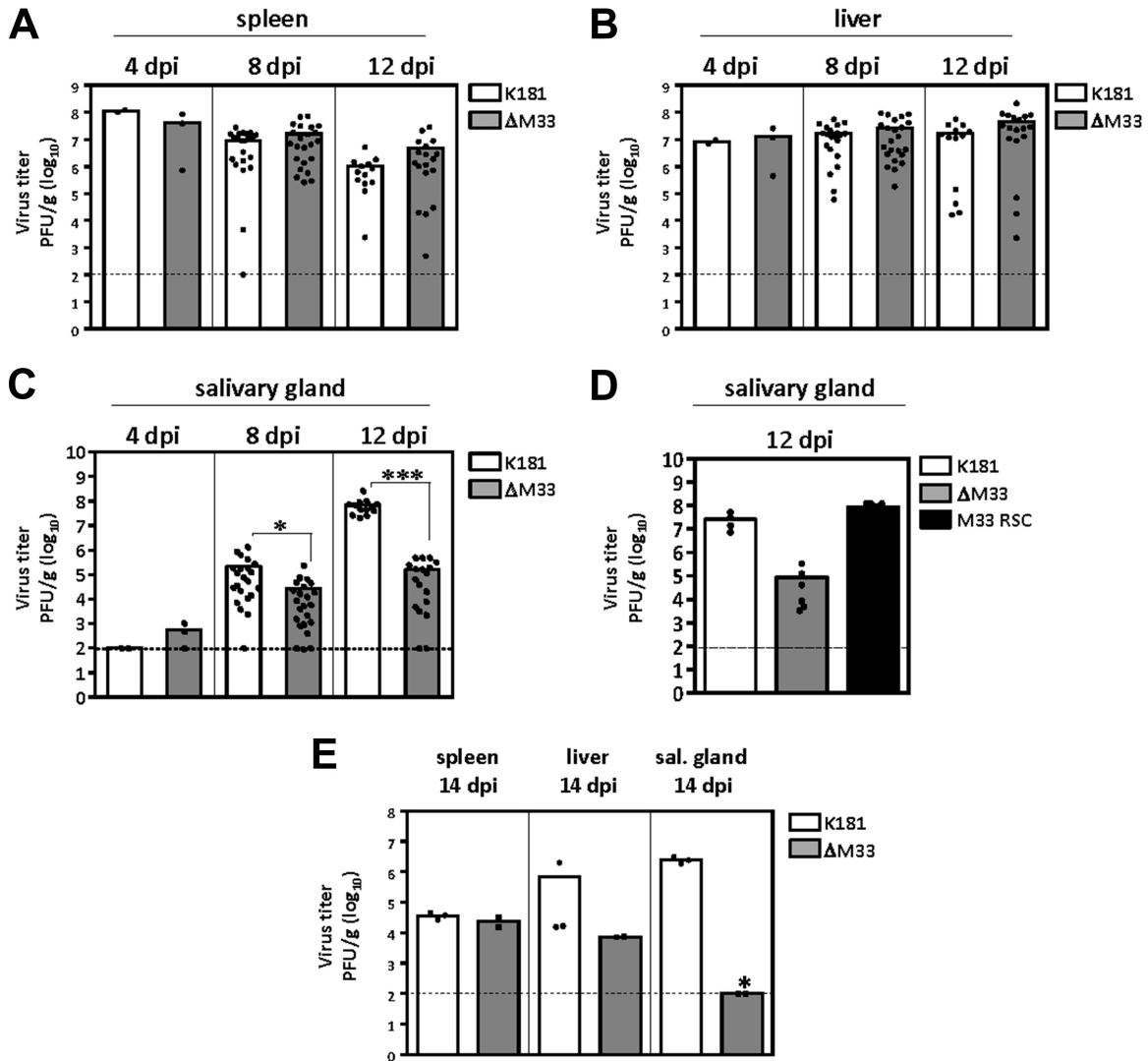
FIG 4 High-dose infection in NSG mice indicates that the ΔM33 virus can reach the salivary gland but fails to replicate efficiently once in the gland. NSG mice were infected intraperitoneally with 1×10^6 PFU of the indicated viruses. At 4, 8, and 12 days postinfection, spleens (A), livers (B), and salivary glands (C, D) were harvested and homogenized with a tissue grinder. (D) Replication of a revertant virus was assessed for salivary gland growth. (E) Virus harvested from the salivary glands at day 12 postinfection was reintroduced into animals via i.p. injection (10^5 PFU per animal). Dilutions of the organ homogenates were used for viral titer determination via plaque assay on NIH 3T3 cell monolayers. Each symbol represents one animal. Dashed lines, the limit of detection. Statistical analyses were performed using an unpaired *t* test. *, $P < 0.05$; ***, $P < 0.001$.

antibodies directed against the immediate early protein M123 (data not shown).

The findings of these immunohistochemical experiments are consistent with our plaque assay-based findings presented in Fig. 4 and indicate that while the number of M44- and M123-positive infected cells is vastly reduced in ΔM33 virus-infected animals, the ΔM33 virus is, in fact, capable of reaching the gland and initiating lytic-phase gene expression. Since the delayed-early protein M44 is expressed, these data suggest that the defect in viral replication exhibited by the ΔM33 virus in the salivary gland is at a step subsequent to the delayed-early phase, possibly at the level of encapsidation, extracellular virion stability, or spread.

Utilization of GFP-tagged virus to examine MCMV spread within the salivary gland. In order to more carefully examine viral replication in salivary glands *in vivo* and gain some insight

into the mechanisms involved in MCMV spread within the gland, we designed K181 and ΔM33 viruses that express GFP. In particular, we chose the GFP approach as we wished to investigate parameters such as intra-acinar spread (movement of virus to adjacent cells within an acinus) and interacinar spread (movement of virus to adjacent or more distal acini). Using this method would enable us to more accurately quantitate the number of MCMV-infected cells at multiple points and enable us to more closely examine cell-cell spread of MCMV within the salivary gland. Basic *in vitro* characterization of these viruses in NIH 3T3 fibroblasts indicated that the newly constructed GFP-tagged viruses (K181-GFP and ΔM33-GFP) replicated with kinetics and titers similar to those of their untagged counterparts (Fig. 6A) (29). Also, GFP expression in infected cells was determined via fluorescence-activated cell sorting, and infection with both K181-GFP virus and ΔM33-GFP virus resulted in high levels of GFP expression,
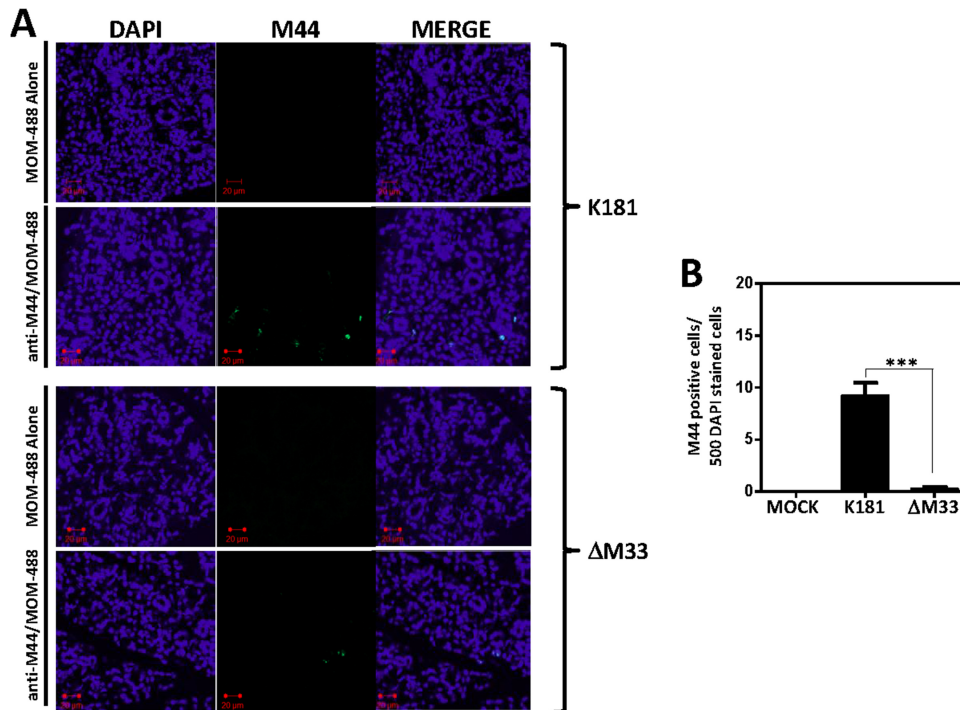
FIG 5 M33-null MCMVs enter the gland but exhibit reduced numbers of early antigen-positive cells. NSG mice were infected intraperitoneally with 1×10^6 PFU of the indicated viruses. At 12 days postinfection, salivary glands were harvested, fixed in 4% paraformaldehyde, and sectioned. Sections of 4 μm were used for immunohistochemistry. (A) K181-infected or ΔM33-infected salivary glands were stained with MOM-488 secondary reagent alone or with anti-M44 MAb plus MOM-488 secondary reagent and mounted in antifade medium containing DAPI. Fluorescence was visualized using an LSM510 two-photon microscope. (B) M44-positive cells were quantified using NIH ImageJ image analysis software, and the graph indicates the number of M44-positive cells per 500 DAPI staining-positive cells. Statistical analyses were performed using an unpaired *t* test. ***, $P < 0.001$.

whereas no GFP expression was obtained after infection with a nontagged K181 virus (data not shown).

To ensure that expression of GFP did not affect the M33 phenotype *in vivo*, NSG mice were infected with a high dose of K181-GFP and ΔM33-GFP viruses (1×10^6 PFU) and viral growth in the spleen and salivary gland was examined (Fig. 6B). Infection with K181-GFP and ΔM33-GFP viruses yielded similar titers in the spleen at 8 and 12 days postinfection. Importantly, analysis of viral growth in the salivary gland again demonstrated that the ΔM33-GFP virus exhibited defective growth in the salivary gland in comparison to that of the K181-GFP virus. This observation is in agreement with the results obtained with the nontagged K181 and ΔM33 viruses, and therefore, the GFP-tagged viruses are appropriate tools to be used to examine viral replication in mouse salivary glands.

Frozen sections of salivary glands infected with either K181-GFP or ΔM33-GFP virus were then analyzed for GFP expression via confocal microscopy. Tile images are shown to facilitate the visualization of large areas of the gland (Fig. 6C and D, top) and higher-magnification images are shown to facilitate the visualization of individual cells (Fig. 6C and D, green boxes). Data are presented for each virus at day 8 postinfection (Fig. 6C) and at day 12 postinfection (Fig. 6D). At 8 days postinfection, in salivary glands infected with K181, about 1 in 50 cells expressed GFP, whereas in the salivary glands of mice infected with ΔM33 virus, GFP expression was detected in approximately 1 in 500 cells and was normally not as intense as K181-GFP expression (Fig. 6C). From day 8 to day 12 there was only a modest increase in the

number of GFP-positive cells for cells infected with either virus (Fig. 6D). Interestingly, the data indicate that neither the K181-GFP virus nor the ΔM33-GFP virus appears to spread focally in the salivary gland in a simple cell-cell fashion, as might be expected on the basis of observations of MCMV spread in cellular monolayers *in vitro*. In particular, at 12 days postinfection, we observed no further development of multicellular infected foci, as would be expected if the virus was spreading to adjacent cells.

M33 is required for efficient viral replication in the salivary glands after bypassing dissemination. Our studies in NOD and NSG mice indicate that the ΔM33 virus reaches the gland but exhibits a reduced replication efficiency once it is in the gland, ultimately leading to decreased viral titers. Thus, our data predict that direct injection of the virus into the gland would result in reduced but detectable viral titers at time points subsequent to the infection. Davis-Poynter et al. performed a similar experiment in the salivary glands of BALB/c mice and did not detect any ΔM33 virus in the glands (28). Their data therefore could not distinguish between the inability to enter the gland or a failure to replicate within the gland. Since our data suggest the latter, we performed intra-salivary gland infections in NOD and NSG mice using K181 and ΔM33 viruses. We observed that following an intra-salivary gland infection of NOD mice, K181 and ΔM33 viruses were detectable in the salivary gland at comparable levels at 4 days postinfection (Fig. 7A). The K181 virus demonstrated a considerable increase in viral titers between 4 and 14 days postinfection, while the ΔM33 virus failed to reach similar viral titers. This resulted in a significant difference in viral titers between wild-type and ΔM33
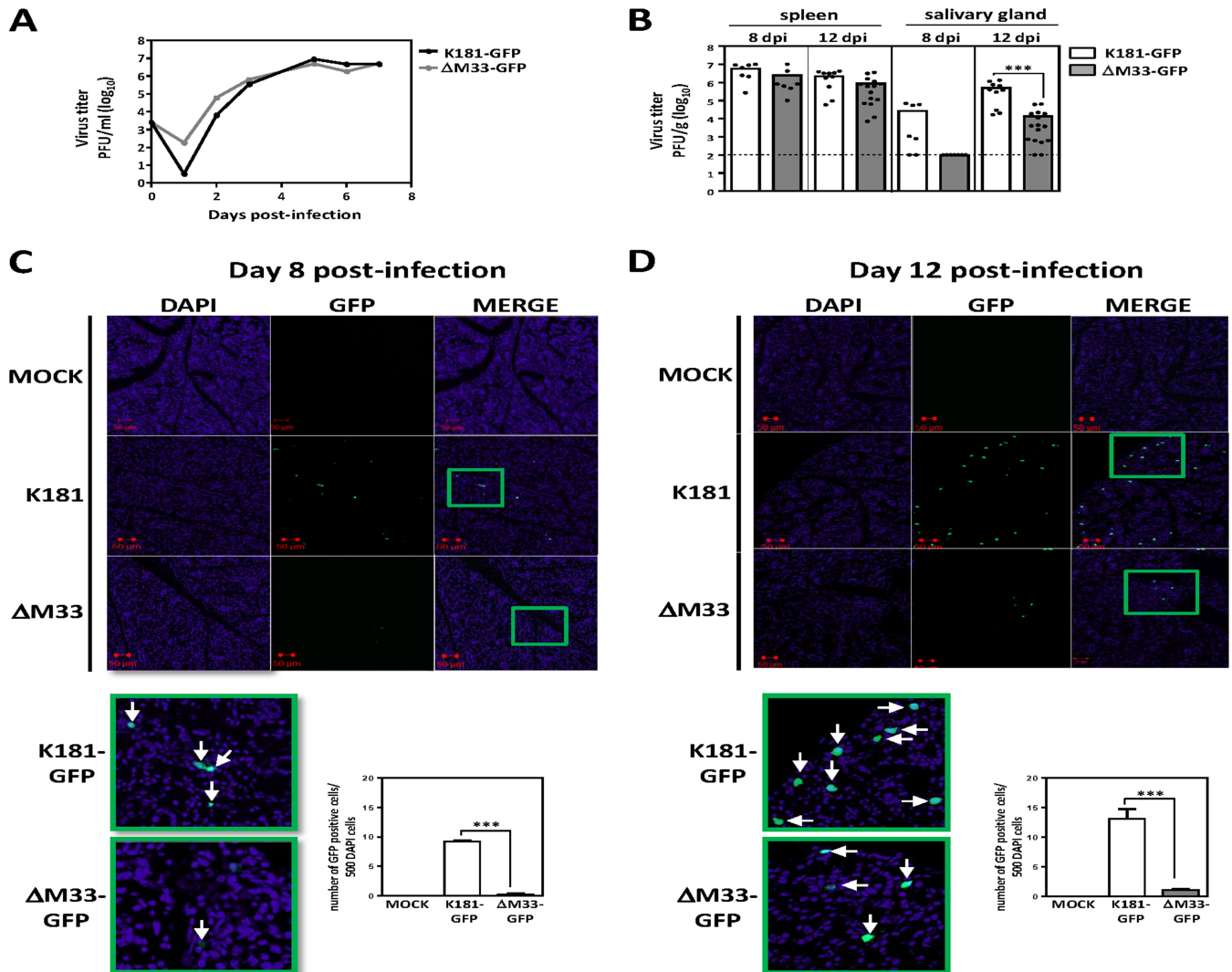
FIG 6 Visualization of MCMV spread in the salivary gland *in vivo* using GFP-tagged viruses. (A) Recombinant viruses expressing GFP were characterized *in vitro* in NIH 3T3 cells to ensure that the inserted GFP cassette did not deleteriously affect replication. NIH 3T3 cells were infected at an MOI of 0.1, and viral titers were determined via plaque assay at the indicated times postinfection. (B) NSG mice were infected intraperitoneally with 1×10^6 PFU of the indicated viruses. At 8 and 12 days postinfection, spleens and salivary glands were harvested and homogenized with a tissue grinder. Dilutions of the organ homogenates were used for viral titer determination via plaque assay on NIH 3T3 cell monolayers. Each symbol represents one animal. (C, D) At day 8 postinfection (C) or day 12 postinfection (D), salivary glands were harvested, fixed in paraformaldehyde, and sectioned. Sections of 4 μm were used for immunohistochemistry. Sections were mounted in antifade medium containing DAPI. Fluorescence was visualized using an LSM510 two-photon microscope. (Bottom) Higher magnification of the areas outlined in green are shown so that single cells (arrows) can be more easily identified. GFP-positive cells were quantified using NIH ImageJ image analysis software, and the graph indicates the number of GFP-positive cells per 500 cells positive by DAPI staining. Statistical analyses were performed using an unpaired *t* test. ***, $P < 0.001$.

viruses at day 14 postinfection (Fig. 7B). Similar results were obtained after intra-salivary gland infection of NSG animals. NSG mice infected with K181 and ΔM33 viruses had equivalent levels of virus in the salivary gland at 4 days postinfection (Fig. 7C). Between days 4 and 14, the wild-type K181 virus demonstrated robust growth in the gland, while the ΔM33 virus demonstrated a reduced propensity to efficiently replicate at this site (Fig. 7D). The observations made using an intra-salivary gland infection approach highlight the requirement for M33 to enable efficient viral amplification in the salivary gland and are consistent with high-dose intraperitoneal infections, as described in Fig. 4.

Wild-type and ΔM33 viruses tagged with GFP were then directly injected into the salivary gland, and at 14 days postinfection, tissue sections were examined for GFP expression (Fig. 8). The distribution of infected cells was visualized by confocal microscopy and enumerated by NIH ImageJ software. The data indicate that cell-free ΔM33 virus is able to enter the acinar epithelial cells but fails to properly spread following an initial round of replication (Fig. 8). Interestingly, the ΔM33 virus exhibited a similar defect when introduced via intraglandular injection or by intraperitoneal infection (Fig. 6 and 8). In the case of the intraglandular infection experiments, cell-free virus has direct access to the glandular epithelium, while in the case of the intraperitoneal infection experiments, virus is disseminated through the bloodstream and introduced into the gland in association with blood leukocytes. In combination, these data indicate that the inability of the virus to
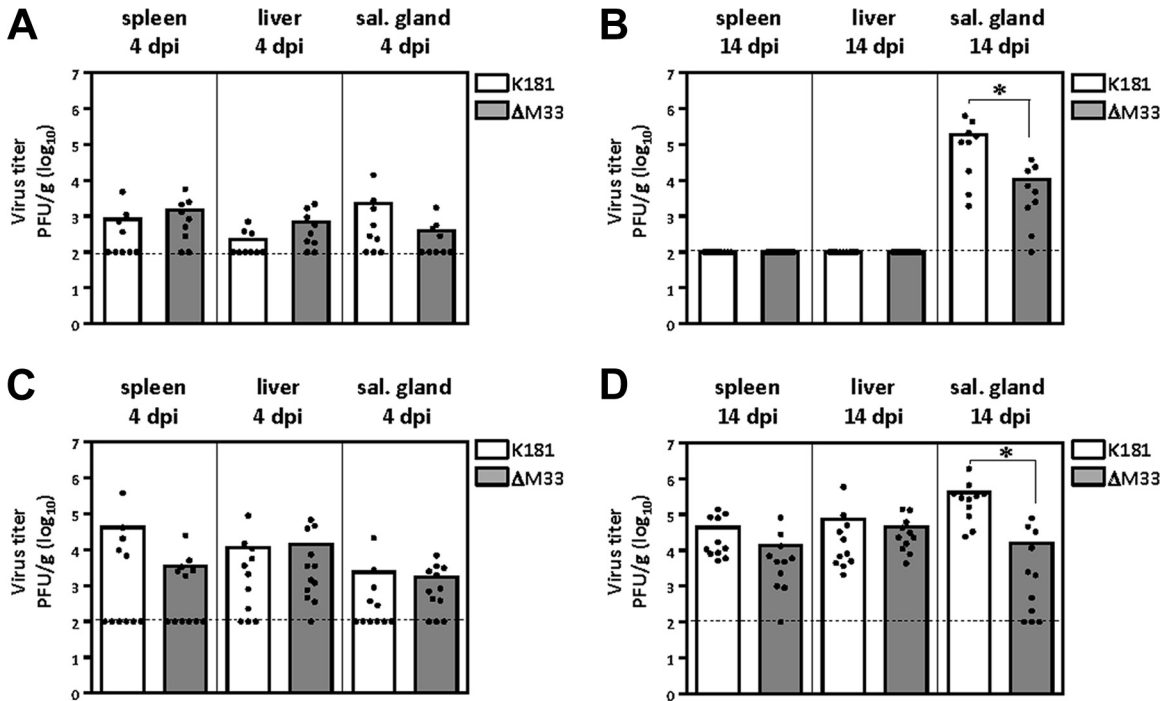
FIG 7 M33 is required for efficient viral replication in the salivary glands after intra-salivary gland injection. NOD (A, B) and NSG (C, D) mice were anesthetized, and 1×10^5 PFU of K181 and ΔM33 viruses was injected in the salivary gland. At 4 days (A, C) and 14 days (B, D) postinfection, salivary glands, spleens, and livers were harvested and homogenized with a tissue grinder. Dilutions of the organ homogenates were used for viral titer determination via plaque assay on NIH 3T3 cell monolayers. Each symbol represents one animal. Dashed lines, the limit of detection. Statistical analyses were performed using an unpaired *t* test. *, $P < 0.05$.

replicate and spread in the salivary gland epithelium is not due to an inherent defect in the ability of ΔM33 virus to transfer from the infected blood leukocytes into the gland.

M33 is dispensable for MCMV replication in primary salivary gland explants grown *ex vivo*. Since ΔM33 viruses replicate

less efficiently once they are localized within the salivary gland *in vivo*, we sought to examine ΔM33 virus replication in primary salivary gland explants *ex vivo*. Salivary glands were excised from 3- to 6-week-old mice and digested with dispase-collagenase, and dissociated cells were allowed to attach to culture plates coated
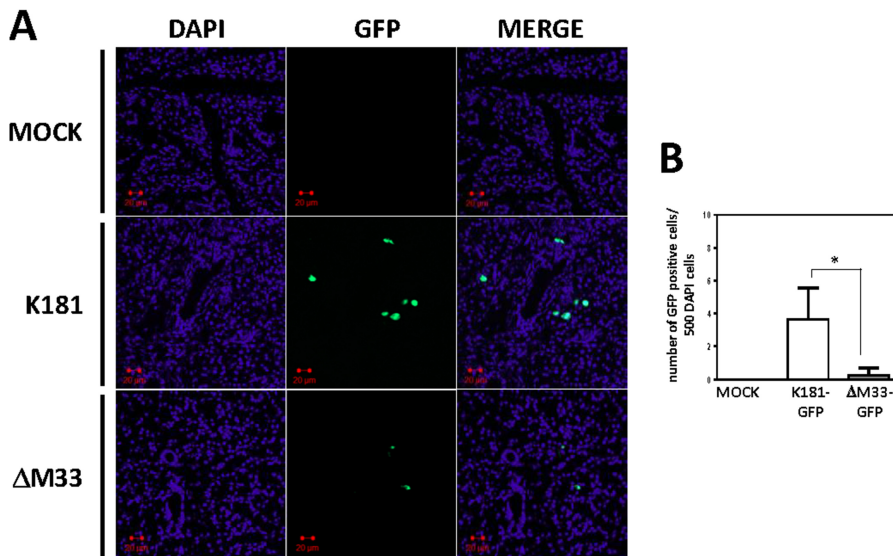

FIG 8 M33 is required for efficient viral spread within the salivary gland epithelium following direct introduction of virus into the gland. NSG mice were anesthetized, and 1×10^5 PFU of GFP-tagged K181 or ΔM33 viruses was injected in the salivary gland. (A) At 14 days postinfection, salivary glands were harvested, fixed in 4% paraformaldehyde, and sectioned. Sections of 4 µm were used for immunohistochemistry. Sections were mounted in antifade medium containing DAPI. Fluorescence was visualized using an LSM510 two-photon microscope. (B) GFP-positive cells were enumerated using NIH ImageJ software. Statistical analyses were performed using an unpaired *t* test. *, $P < 0.05$.

with Cultrex basement membrane extract. Cells were cultured in BEGM medium, which resulted in the outgrowth of clusters of E-cadherin- and ZO-1-positive epithelial cells by days 3 to 5 postisolation (Fig. 9A). RT-PCR analysis of the *ex vivo*-grown clusters indicated that these cells express the acinar cell markers aquaporin 5 (AQP5) and amylase 1 (Amy1), consistent with the epithelial origin of these salivary gland explants (Fig. 9B). Primary salivary gland explant cultures were then infected at 3 to 5 days postisolation with K181 or ΔM33 viruses at an MOI of 0.1, supernatant was collected at days 1 through 4 postinfection, and the viral titers in the supernatants were quantified by plaque assay. We observed that ΔM33 virus replicated to levels similar to those of K181 virus in primary cells infected *ex vivo* (Fig. 9C). Thus, while the ΔM33 virus failed to replicate efficiently in salivary gland cells contained within the three-dimensional structure of the gland *in vivo*, it replicated efficiently in primary salivary gland cells grown as cell clusters *ex vivo*.

Examination of MCMV infection and spread in the salivary gland explants indicated that the virus infected the salivary gland explant cell clusters and that both K181-GFP and ΔM33-GFP viruses spread efficiently to adjacent cells within the clusters, creating multicellular focal plaques (Fig. 9D), in sharp contrast to what we observed with MCMV spread within the gland *in vivo* (Fig. 6 and 8). Salivary gland clusters are outlined in red in Fig. 9D to help with the visualization of the infection and spread of GFP-tagged viruses. Taken together, the results of our studies are consistent with a model in which M33 is essential for robust interacinar spread in the salivary gland *in vivo* but dispensable for intercellular spread in salivary gland epithelial cells grown *in vitro*.

DISCUSSION

In this study, we used an immunocompromised animal model that enabled us to examine the replication of the ΔM33 virus within the mouse salivary gland, which was not possible with immunocompetent strains of mice. Using this model, we determined that the ΔM33 virus exhibits a significant growth defect of over 400-fold in the gland compared with the growth of the wild-type virus. We also provide evidence that M33 is not required for viral cell-associated dissemination from the primary replication sites to the salivary gland, as the numbers of blood leukocytes infected with K181 or ΔM33 viruses were similar. Moreover, from the use of a combination of direct salivary gland injection experiments, *in vitro* replication studies with isolated primary salivary gland explants, and assessment of intraglandular viral spread with GFP-tagged viruses, we conclude that the ΔM33 virus exhibits a defect in interacinar spread, thus preventing efficient viral growth in the gland.

The NSG strain is derived from the NOD strain and has been used in other studies with infectious disease agents, including CMV and HIV (45–47). NSG animals have impaired innate NK function and adaptive T and B cell function, have significantly impaired cytokine signaling activity, and are thought to be the most severely immunocompromised animals available (38). We initially sought to use the NSG model in our studies to determine whether M33 functions in an immunomodulatory manner and determine if the salivary gland defect exhibited by the ΔM33 virus would be rescued or normalized in the NSG mice. Additionally, we hypothesized that by removing innate and adaptive immunity, MCMV infection in NSG animals would result in higher and more sustained virus titers in primary infected organs and in blood and

perhaps lead to the increased movement of ΔM33 virus to the salivary glands. While it is clear that the growth of the ΔM33 virus is not fully rescued to wild-type levels in the NSG animals deficient for T, B, and NK cell control, this approach did enable the ΔM33 virus to reach the gland, thus facilitating our studies, from which we conclude that the ΔM33 virus exhibits a defect in growth within the gland itself. This conclusion that the ΔM33 virus exhibits a defect within the gland itself was not achievable in prior studies, as it was not possible to detect any amount of ΔM33 virus in the gland to establish a baseline from which one could assess how much the virus grows relative to the level of virus present at baseline (28, 29, 33–35). We cannot rule out the possibility, however, that M33 may also play a role in manipulating some aspect of immune function that, when absent in the NSG animals, enables the virus to move more efficiently to the gland.

In addition to the profound phenotype regarding the deficient salivary gland growth of ΔM33 virus that was observed, previous studies reported that disruption of M33 resulted in more rapid clearance of virus from the spleens of BALB/c mice, which in turn could result in decreased viral dissemination to distal sites, such as the salivary gland (34, 35). Our experiments in NOD mice demonstrate that while the ΔM33 virus was unable to grow in the salivary gland after an intraperitoneal infection, both wild-type and ΔM33 viruses were present at similar levels in spleen at 7 days postinfection and, likewise, were cleared from this organ by 14 days postinfection. Therefore, while it is possible that M33 may affect viral clearance from the spleen under some experimental conditions and in some mouse strains, our data indicate that the clearance of the ΔM33 virus from initial sites of infection, like the spleen, is not directly responsible for the subsequent growth defect of ΔM33 viruses within distal organs like the salivary gland.

The precise mechanism for how M33 activity results in increased growth within the gland is currently unknown. *In vitro* signaling studies by us and others have demonstrated that M33 is a $G\alpha_{q/11}$-coupled G protein-coupled receptor that signals through a classical inositol 1,4,5-triphosphate-generating signaling pathway, leading to the activation of PKC and a number of transcription factors (29, 30, 32). Evidence for coupling to $G\alpha_{q/11}$ in these *in vitro* studies comes from using mouse embryonic fibroblasts devoid of $G\alpha_{q/11}$ (32). The motif in M33 responsible for coupling to G proteins has been identified to be amino acids 130 to 132 (Asp-Arg-Tyr), and importantly, recombinant MCMVs expressing an M33 variant in which arginine 131 has been mutated to alanine are unable to grow in the salivary gland (29, 33). Thus, it is clear that G-protein coupling is essential for salivary gland growth, but whether $G\alpha_{q/11}$ is truly required for *in vivo* function remains unclear. Experiments aimed at defining a requirement for M33 coupling to $G\alpha_{q/11}$ are difficult, as $G\alpha_{q/11}$-null animals do not live past fetal day 11.5 (48). Our current studies provide a basis from which to now examine this question, as we have localized the M33 defect to within the salivary gland. Using tissue-specific CRE expression should enable the selective knockout of $G\alpha_{q/11}$ proteins in the gland and obtain an answer to this question (49, 50).

It is interesting that MCMV spread within the gland *in vivo* does not appear to involve the transfer of virus to adjacent cells within a particular acinus (intra-acinar spread), as we rarely found multicellular foci exhibiting GFP expression. This is in sharp contrast to how the virus spreads in cell culture, where the virus can easily spread to adjacent cells during the development of an individual plaque. It remains unclear how the cell-cell junctions form
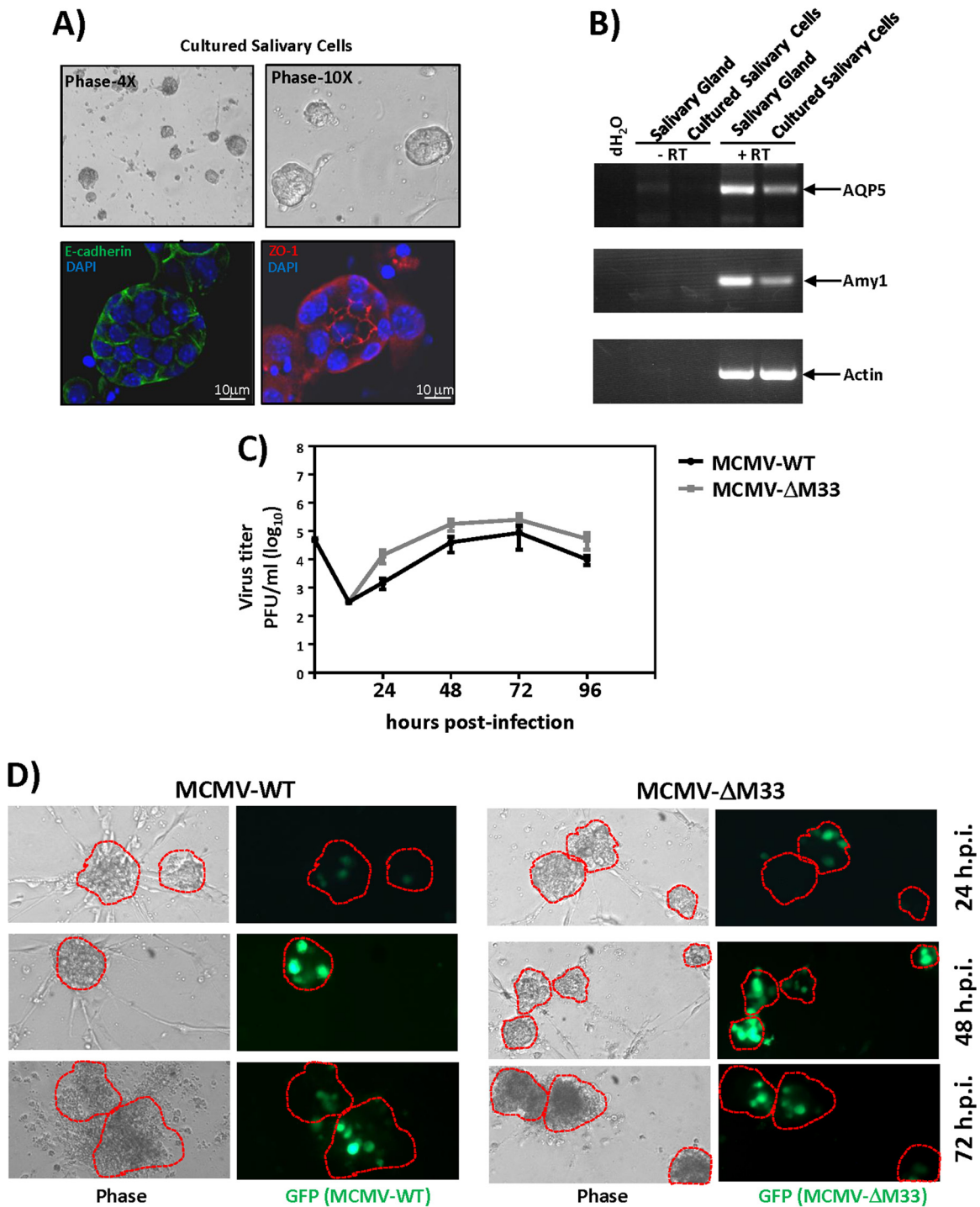
FIG 9 M33 is not required for viral replication in primary salivary gland explants infected *in vitro*. (A) Salivary glands were harvested from 3- to 6-week-old mice, dispersed via dispase-collagenase digestion, plated in culture plates coated with Cultrex basement membrane extract, and grown in BEGM medium. These growth conditions led to the outgrowth of tight clusters (6 to 20 cells per cluster) of primary salivary gland cells (top). Staining of these clusters with E-cadherin antibody demonstrates uniform staining at the plasma membrane of each cell in these clusters (bottom left). Staining with ZO-1 antibodies demonstrates localization of the protein at cell-cell junctions primarily toward the inner part of the clusters (bottom right). (B) cDNA was prepared with an iScript cDNA synthesis kit (Bio-Rad), and mRNA expression was examined via PCR with primers specific for AQP5, Amy1, and β-actin. dH$_2$O, distilled H$_2$O; Salivary gland, RNA directly isolated from salivary gland tissue. (C) Salivary gland clusters were then infected with wild-type (WT) MCMV (K181) or MCMV with an M33 deletion (ΔM33) at an MOI of 0.1. The cellular supernatant was harvested at the indicated times postinfection, and dilutions of cell supernatants were used for viral titer determination via plaque assay on NIH 3T3 cell monolayers. (D) K181-GFP and ΔM33-GFP infection and spread in primary derived salivary gland clusters at the indicated times postinfection. h.p.i., hours postinfection. Phase, phase-contrast microscopy.

in vivo in the gland and if they prevent infection via adjacent cells or if the polarized nature of the acinar cells directs viral release from the apical membranes. The main biological function of the salivary gland acinar epithelial cells is to secrete H_2O, electrolytes, and proteinaceous components of the saliva, so it is seems likely that MCMV release from the salivary gland epithelial cells may use some component of the secretion machinery (51). Studies aimed at analyzing MCMV spread within the salivary gland in animals deficient in channel activity or in signaling components regulating channel activity should provide important insight into the mechanism of MCMV spread within the gland.

In summary, we have shown that the GPCR M33 of MCMV is not required for viral growth at sites of acute infection or for hematogenous dissemination within the host; however, we now demonstrate that M33 is required for growth within the salivary gland itself and provide evidence supporting the hypothesis that M33 is required for the interacinar movement of virus within the gland. Considering that salivary glands are a site for viral persistence and critical to horizontal transmission, the understanding of the requirements of M33 and M33 signaling for viral replication at this site could lead to new therapeutic treatments intended to control viral transmission and disease.

ACKNOWLEDGMENTS

REFERENCES

1. **Cannon MJ, Schmid DS, Hyde TB.** 2010. Review of cytomegalovirus seroprevalence and demographic characteristics associated with infection. Rev. Med. Virol. **20:**202–213. http://dx.doi.org/10.1002/rmv.655.
2. **Manicklal S, Emery VC, Lazzarotto T, Boppana SB, Gupta RK.** 2013. The "silent" global burden of congenital cytomegalovirus. Clin. Microbiol. Rev. **26:**86–102. http://dx.doi.org/10.1128/CMR.00062-12.
3. **Grosse SD, Ross DS, Dollard SC.** 2008. Congenital cytomegalovirus (CMV) infection as a cause of permanent bilateral hearing loss: a quantitative assessment. J. Clin. Virol. **41:**57–62. http://dx.doi.org/10.1016/j.jcv.2007.09.004.
4. **Dollard SC, Grosse SD, Ross DS.** 2007. New estimates of the prevalence of neurological and sensory sequelae and mortality associated with congenital cytomegalovirus infection. Rev. Med. Virol. **17:**355–363. http://dx.doi.org/10.1002/rmv.544.
5. **Rubin RH.** 2001. Cytomegalovirus in solid organ transplantation. Transpl. Infect. Dis. **3**(Suppl 2):S1–S5. http://dx.doi.org/10.1034/j.1399-3062.2001.00001.x.
6. **Eid AJ, Razonable RR.** 2010. New developments in the management of cytomegalovirus infection after solid organ transplantation. Drugs **70:** 965–981. http://dx.doi.org/10.2165/10898540-000000000-00000.
7. **Scalzo AA, Corbett AJ, Rawlinson WD, Scott GM, Degli-Esposti MA.** 2007. The interplay between host and viral factors in shaping the outcome of cytomegalovirus infection. Immunol. Cell Biol. **85:**46–54. http://dx.doi.org/10.1038/sj.icb.7100013.
8. **Sacher T, Mohr CA, Weyn A, Schlichting C, Koszinowski UH, Ruzsics Z.** 2012. The role of cell types in cytomegalovirus infection in vivo. Eur. J. Cell Biol. **91:**70–77. http://dx.doi.org/10.1016/j.ejcb.2011.02.002.
9. **Handke W, Krause E, Brune W.** 2012. Live or let die: manipulation of cellular suicide programs by murine cytomegalovirus. Med. Microbiol. Immunol. **201:**475–486. http://dx.doi.org/10.1007/s00430-012-0264-z.
10. **Cekinovic D, Lisnic VJ, Jonjic S.** 2014. Rodent models of congenital cytomegalovirus infection. Methods Mol. Biol. **1119:**289–310. http://dx.doi.org/10.1007/978-1-62703-788-4_16.
11. **Collins TM, Quirk MR, Jordan MC.** 1994. Biphasic viremia and viral gene expression in leukocytes during acute cytomegalovirus infection of mice. J. Virol. **68:**6305–6311.
12. **Bale JF, Jr, O'Neil ME.** 1989. Detection of murine cytomegalovirus DNA in circulating leukocytes harvested during acute infection of mice. J. Virol. **63:**2667–2673.
13. **Hsu KM, Pratt JR, Akers WJ, Achilefu SI, Yokoyama WM.** 2009. Murine cytomegalovirus displays selective infection of cells within hours after systemic administration. J. Gen. Virol. **90:**33–43. http://dx.doi.org/10.1099/vir.0.006668-0.
14. **Sacher T, Podlech J, Mohr CA, Jordan S, Ruzsics Z, Reddehase MJ, Koszinowski UH.** 2008. The major virus-producing cell type during murine cytomegalovirus infection, the hepatocyte, is not the source of virus dissemination in the host. Cell Host Microbe **3:**263–272. http://dx.doi.org/10.1016/j.chom.2008.02.014.
15. **Sacher T, Andrassy J, Kalnins A, Dolken L, Jordan S, Podlech J, Ruzsics Z, Jauch KW, Reddehase MJ, Koszinowski UH.** 2011. Shedding light on the elusive role of endothelial cells in cytomegalovirus dissemination. PLoS Pathog. **7:**e1002366. http://dx.doi.org/10.1371/journal.ppat.1002366.
16. **Campbell AE, Cavanaugh VJ, Slater JS.** 2008. The salivary glands as a privileged site of cytomegalovirus immune evasion and persistence. Med. Microbiol. Immunol. **197:**205–213. http://dx.doi.org/10.1007/s00430-008-0077-2.
17. **Henson D, Strano AJ.** 1972. Mouse cytomegalovirus. Necrosis of infected and morphologically normal submaxillary gland acinar cells during termination of chronic infection. Am. J. Pathol. **68:**183–202.
18. **Humphreys IR, de Trez C, Kinkade A, Benedict CA, Croft M, Ware CF.** 2007. Cytomegalovirus exploits IL-10-mediated immune regulation in the salivary glands. J. Exp. Med. **204:**1217–1225. http://dx.doi.org/10.1084/jem.20062424.
19. **Krmpotic A, Bubic I, Polic B, Lucin P, Jonjic S.** 2003. Pathogenesis of murine cytomegalovirus infection. Microbes Infect. **5:**1263–1277. http://dx.doi.org/10.1016/j.micinf.2003.09.007.
20. **Jonjic S, Mutter W, Weiland F, Reddehase MJ, Koszinowski UH.** 1989. Site-restricted persistent cytomegalovirus infection after selective long-term depletion of $CD4^+$ T lymphocytes. J. Exp. Med. **169:**1199–1212. http://dx.doi.org/10.1084/jem.169.4.1199.
21. **Reddehase MJ, Mutter W, Munch K, Buhring HJ, Koszinowski UH.** 1987. CD8-positive T lymphocytes specific for murine cytomegalovirus immediate-early antigens mediate protective immunity. J. Virol. **61:**3102–3108.
22. **Jonjic S, Pavic I, Lucin P, Rukavina D, Koszinowski UH.** 1990. Efficacious control of cytomegalovirus infection after long-term depletion of $CD8^+$ T lymphocytes. J. Virol. **64:**5457–5464.
23. **Walton SM, Mandaric S, Torti N, Zimmermann A, Hengel H, Oxenius A.** 2011. Absence of cross-presenting cells in the salivary gland and viral immune evasion confine cytomegalovirus immune control to effector CD4 T cells. PLoS Pathog. **7:**e1002214. http://dx.doi.org/10.1371/journal.ppat.1002214.
24. **Fleming P, Davis-Poynter N, Degli-Esposti M, Densley E, Papadimitriou J, Shellam G, Farrell H.** 1999. The murine cytomegalovirus chemokine homolog, m131/129, is a determinant of viral pathogenicity. J. Virol. **73:**6800–6809.
25. **Hanson LK, Slater JS, Karabekian Z, Ciocco-Schmitt G, Campbell AE.** 2001. Products of US22 genes M140 and M141 confer efficient replication of murine cytomegalovirus in macrophages and spleen. J. Virol. **75:**6292–6302.
26. **Fleming P, Kvansakul M, Voigt V, Kile BT, Kluck RM, Huang DC, Degli-Esposti MA, Andoniou CE.** 2013. MCMV-mediated inhibition of the pro-apoptotic Bak protein is required for optimal in vivo replication. PLoS Pathog. **9:**e1003192. http://dx.doi.org/10.1371/journal.ppat.1003192.
27. **Lagenaur LA, Manning WC, Vieira J, Martens CL, Mocarski ES.** 1994. Structure and function of the murine cytomegalovirus sgg1 gene: a determinant of viral growth in salivary gland acinar cells. J. Virol. **68:**7717–7727.
28. **Davis-Poynter NJ, Lynch DM, Vally H, Shellam GR, Rawlinson WD, Barrell BG, Farrell HE.** 1997. Identification and characterization of a G protein-coupled receptor homolog encoded by murine cytomegalovirus. J. Virol. **71:**1521–1529.
29. **Sherrill JD, Stropes MP, Schneider OD, Koch DE, Bittencourt FM, Miller JL, Miller WE.** 2009. Activation of intracellular signaling pathways

by the murine cytomegalovirus G protein-coupled receptor M33 occurs via PLC-β/PKC-dependent and -independent mechanisms. J. Virol. **83:** 8141–8152. http://dx.doi.org/10.1128/JVI.02116-08.

30. **Waldhoer M, Kledal TN, Farrell H, Schwartz TW.** 2002. Murine cytomegalovirus (CMV) M33 and human CMV US28 receptors exhibit similar constitutive signaling activities. J. Virol. **76:**8161–8168. http://dx.doi.org/10.1128/JVI.76.16.8161-8168.2002.

31. **Melnychuk RM, Smith P, Kreklywich CN, Ruchti F, Vomaske J, Hall L, Loh L, Nelson JA, Orloff SL, Streblow DN.** 2005. Mouse cytomegalovirus M33 is necessary and sufficient in virus-induced vascular smooth muscle cell migration. J. Virol. **79:**10788–10795. http://dx.doi.org/10.1128/JVI.79.16.10788-10795.2005.

32. **Sherrill JD, Miller WE.** 2006. G protein-coupled receptor (GPCR) kinase 2 regulates agonist-independent Gq/11 signaling from the mouse cytomegalovirus GPCR M33. J. Biol. Chem. **281:**39796–39805. http://dx.doi.org/10.1074/jbc.M610026200.

33. **Case R, Sharp E, Benned-Jensen T, Rosenkilde MM, Davis-Poynter N, Farrell HE.** 2008. Functional analysis of the murine cytomegalovirus chemokine receptor homologue M33: ablation of constitutive signaling is associated with an attenuated phenotype in vivo. J. Virol. **82:**1884–1898. http://dx.doi.org/10.1128/JVI.02550-06.

34. **Cardin RD, Schaefer GC, Allen JR, Davis-Poynter NJ, Farrell HE.** 2009. The M33 chemokine receptor homolog of murine cytomegalovirus exhibits a differential tissue-specific role during in vivo replication and latency. J. Virol. **83:**7590–7601. http://dx.doi.org/10.1128/JVI.00386-09.

35. **Farrell HE, Abraham AM, Cardin RD, Sparre-Ulrich AH, Rosenkilde MM, Spiess K, Jensen TH, Kledal TN, Davis-Poynter N.** 2011. Partial functional complementation between human and mouse cytomegalovirus chemokine receptor homologues. J. Virol. **85:**6091–6095. http://dx.doi.org/10.1128/JVI.02113-10.

36. **Farrell HE, Abraham AM, Cardin RD, Molleskov-Jensen AS, Rosenkilde MM, Davis-Poynter N.** 2013. Identification of common mechanisms by which human and mouse cytomegalovirus seven-trans membrane receptor homologues contribute to in vivo phenotypes in a mouse model. J. Virol. **87:**4112–4117. http://dx.doi.org/10.1128/JVI.03406-12.

37. **Shultz LD, Brehm MA, Garcia-Martinez JV, Greiner DL.** 2012. Humanized mice for immune system investigation: progress, promise and challenges. Nat. Rev. Immunol. **12:**786–798. http://dx.doi.org/10.1038/nri3311.

38. **Shultz LD, Lyons BL, Burzenski LM, Gott B, Chen X, Chaleff S, Kotb M, Gillies SD, King M, Mangada J, Greiner DL, Handgretinger R.** 2005. Human lymphoid and myeloid cell development in NOD/LtSz-scid IL2R gamma null mice engrafted with mobilized human hemopoietic stem cells. J. Immunol. **174:**6477–6489. http://dx.doi.org/10.4049/jimmunol.174.10.6477.

39. **Cao X, Shores EW, Hu-Li J, Anver MR, Kelsall BL, Russell SM, Drago J, Noguchi M, Grinberg A, Bloom ET, Paul WE, Katz SI, Love PE,** Leonard WJ. 1995. Defective lymphoid development in mice lacking expression of the common cytokine receptor gamma chain. Immunity **2:**223–238. http://dx.doi.org/10.1016/1074-7613(95)90047-0.

40. **Loh LC, Balachandran N, Britt WJ.** 1991. Characterization of a membrane-associated phosphoprotein of murine cytomegalovirus (pp50) and its immunological cross-reactivity with a human cytomegalovirus protein. Virology **183:**181–194. http://dx.doi.org/10.1016/0042-6822(91)90131-T.

41. **Trgovcich J, Stimac D, Polic B, Krmpotic A, Pernjak-Pugel E, Tomac J, Hasan M, Wraber B, Jonjic S.** 2000. Immune responses and cytokine induction in the development of severe hepatitis during acute infections with murine cytomegalovirus. Arch. Virol. **145:**2601–2618. http://dx.doi.org/10.1007/s007050070010.

42. **Janebodin K, Buranaphatthana W, Ieronimakis N, Hays AL, Reyes M.** 2013. An in vitro culture system for long-term expansion of epithelial and mesenchymal salivary gland cells: role of TGF-beta1 in salivary gland epithelial and mesenchymal differentiation. Biomed. Res. Int. **2013:**815895. http://dx.doi.org/10.1155/2013/815895.

43. **Upton JW, Kaiser WJ, Mocarski ES.** 2010. Virus inhibition of RIP3-dependent necrosis. Cell Host Microbe **7:**302–313. http://dx.doi.org/10.1016/j.chom.2010.03.006.

44. **Jordan MC, Takagi JL.** 1983. Virulence characteristics of murine cytomegalovirus in cell and organ cultures. Infect. Immun. **41:**841–843.

45. **Livingston-Rosanoff D, Daley-Bauer LP, Garcia A, McCormick AL, Huang J, Mocarski ES.** 2012. Antiviral T cell response triggers cytomegalovirus hepatitis in mice. J. Virol. **86:**12879–12890. http://dx.doi.org/10.1128/JVI.01752-12.

46. **Smith MS, Goldman DC, Bailey AS, Pfaffle DL, Kreklywich CN, Spencer DB, Othieno FA, Streblow DN, Garcia JV, Fleming WH, Nelson JA.** 2010. Granulocyte-colony stimulating factor reactivates human cytomegalovirus in a latently infected humanized mouse model. Cell Host Microbe **8:**284–291. http://dx.doi.org/10.1016/j.chom.2010.08.001.

47. **Balazs AB, Chen J, Hong CM, Rao DS, Yang L, Baltimore D.** 2012. Antibody-based protection against HIV infection by vectored immunoprophylaxis. Nature **481:**81–84. http://dx.doi.org/10.1038/nature10660.

48. **Offermanns S, Zhao LP, Gohla A, Sarosi I, Simon MI, Wilkie TM.** 1998. Embryonic cardiomyocyte hypoplasia and craniofacial defects in G alpha q/G alpha 11-mutant mice. EMBO J. **17:**4304–4312. http://dx.doi.org/10.1093/emboj/17.15.4304.

49. **Nagy A, Mar L, Watts G.** 2009. Creation and use of a Cre recombinase transgenic database. Methods Mol. Biol. **530:**365–378. http://dx.doi.org/10.1007/978-1-59745-471-1_19.

50. **Kos CH.** 2004. Cre/loxP system for generating tissue-specific knockout mouse models. Nutr. Rev. **62:**243–246. http://dx.doi.org/10.1111/j.1753-4887.2004.tb00046.x.

51. **Carpenter GH.** 2013. The secretion, components, and properties of saliva. Annu. Rev. Food Sci. Technol. **4:**267–276. http://dx.doi.org/10.1146/annurev-food-030212-182700.